Single-molecule magnet behaviour in a Dy(III) pentagonal bipyramidal complex with a quasi linear Cl-Dy-Cl sequence.

Jérôme Long*,[a] Alexander N. Selikhov,[b] Ekaterina Mamontova,[a] Konstantin A. Lyssenko,[c] Yannick Guari,[a] Joulia Larionova[a] and Alexander A. Trifonov*[b,c]

We report the synthesis and magnetic investigations of a dysprosium pentagonal bipyramidal complex $[Dy(THF)_5Cl_2][BPh_4]$ (1) exhibiting a linear Cl-Dy-Cl sequence suitable to provide a coordination environment allowing a zero-field slow relaxation of the magnetization. Besides, the complex shows also a dual luminescence originating from $[BPh_4]^-$ and Dy^{3+}.

The ability for a coordination complex to present bistable magnetic states continues to catch attention of chemists and physicists since the discovery of this phenomenon nearly thirty years ago.[1-2] In this sense, the field of Single-Molecule Magnets (SMM) has taken an upturn with the use of lanthanide ions to design highly magnetically anisotropic complexes exhibiting exceptional performances,[3-6] making such molecular systems as potential candidates for applications in data storage, spintronics or quantum computing.[3, 7-9] In lanthanide SMM, the occurrence of a slow relaxation of the magnetization is directly correlated to the lanthanide crystal-field generated by the surrounding ligands that favours the creation of an anisotropic barrier, Δ, opposing two antiparallel directions of the magnetic moment ($\pm m_J$). Intuitive synthetic strategies based on simple electrostatic considerations have been therefore applied to exploit the intrinsic magnetic anisotropy of 4*f* ions and engineer complexes displaying high energy barriers and blocking temperatures. Hence, one of the basic principles consists in stabilizing at most the electronic density of the 4*f* orbitals with a defined distribution of the negatively charged ligands.[10] This implies that oblate electronic density is efficiently stabilized by axial crystal-field, while prolate one demands an equatorial crystal-field. Such approach simultaneously increases the crystal-field splitting and minimizes the Quantum Tunnelling of the Magnetization (QTM), which provides direct relaxation within the ground state doublet. In addition to the relaxation of the magnetization through the first or higher excited states, systems with optimized molecular vibrations have to be engineered in order to reduce the spin-phonon coupling that induces alternative pathways (Raman or direct process) that clearly demand to be further comprehended.[3-6, 11]

One of the most relevant approaches to design performing Dy^{3+}-based SMM consists in stabilizing the Dy^{3+} oblate electronic density by two ligands with high electronic density in axial positions and eventually other weak donor ligands in an equatorial plane. [6, 12] Indeed major breakthroughs in this field have recently been achieved by using coordination and organometallic chemistry [13-18] that have pushed back the limits to reach a magnetic hysteresis up to 60 K in a dysprosium metallocene complex[19-20].

On the other hand, it was shown that engineering pseudo-linear complexes using simple coordination chemistry ligands is far to be straightforward owing to the difficulty to accurately control the crystal-field and symmetry around the lanthanide site. In this sense, all the aforementioned examples[13-20] used either negatively charged oxygen or organometallic based-ligands. Surprisingly, chloride ion has been only rarely used to design complexes showing a linear Cl-Dy-Cl sequence[21-22] although it is known as the third most electronegative element after fluorine and oxygen.

With this in mind, we report herein the synthesis, structure and magnetic studies of a dysprosium(III) dichloride pentagonal bipyramidal complex exhibiting a linear Cl-Dy-Cl sequence. The complex exhibits a zero-field slow relaxation of the magnetization associated with a genuine SMM behaviour and a dual luminescence.

Our design strategy relies on the formation of a cationic $[DyCl_2]^+$ moiety in association with a bulky anion to favour its crystallization. Thus, the reaction between $DyCl_3$ and $NaBPh_4$ was carried out in THF at room temperature in anhydrous conditions and allowed to obtain single crystals of $[DyCl_2(THF)_5][B(C_6H_5)_4]\cdot 0.5(THF)$ (**1**) (Scheme S1) after slow diffusion of hexane.

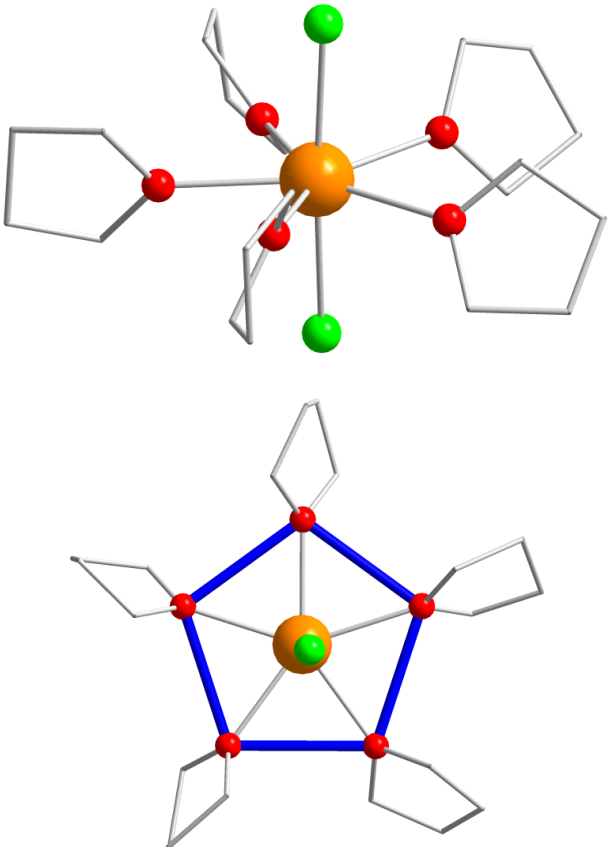

Fig. 1. Top: Molecular structure of one of the independent complex $[DyCl_2(THF)_5]^+$ in **1**. Colour code: orange, Dy; red, O; grey, C; green, Cl. Hydrogen atoms have been omitted for clarity. Bottom: View showing the pentagonal bipyramidal arrangement.

The molecular structure obtained by X-Ray diffraction on single-crystal indicates that **1** crystallizes in the triclinic $P\bar{1}$ space group with two crystallographically independent complexes (noted Dy1 and Dy2) within the asymmetric unit. The coordination environment of both Dy^{3+} sites is composed of two coordinated chlorides located in a *trans* fashion, as well as of five THF ligands in an equatorial plane leading to a seven coordination number (Fig. 1). The Dy-Cl distances, ranging from 2.562(1) to 2.587(1) Å, are significantly longer than the Dy-O ones comprised between 2.376(3) and 2.416(3) Å. The observed geometrical parameters in **1** are rather close to those found in the $[DyCl_2(THF)_5][DyCl_4(THF)_2]$ complex.[23] The coordination geometry for both Dy^{3+} sites was quantitatively analyzed with the SHAPE[24] software, which shows that it is a slightly distorted pentagonal bipyramidal (Table S1). The distortion of the polyhedron is due to a deviation of the Cl-Dy-Cl angle from the linearity (175.90(3) and 179.68(3)°), as well as puckering of the DyO_5 equatorial plane. Crystal packing analysis (Fig. S1, ESI) reveals the presence of C-H···Cl hydrogen bonds involving the tetraphenylborate moieties, while the shortest Dy^{3+}-Dy^{3+} is equal to 8.9345(8) Å.

The magnetic properties of **1** were investigated in both, static and dynamic modes by using a SQUID MPMS-XL. At 300 K, the χT value of 14.20 $cm^3.K.mol^{-1}$ is in good accordance with the value of 14.17 $cm^3.K.mol^{-1}$ ($^6H_{15/2}$) expected for a unique Dy^{3+} ion using the free-ion approximation. Lowering the temperature results in a monotonous decrease of χT due to the thermal depopulation of the m_J levels before dropping for temperature lower than 12 K (Fig. S2). The field dependence of the magnetization at 1.8 K shows a value of 6.08 *N*β under à 70 kOe field and does not show any saturation confirming the presence of a magnetic anisotropy (Fig. S2). Besides, a sigmoidal shape is present at low fields, which has been ascribed in other systems to the occurrence of the high anisotropy or magnetic blocking.[14, 17]

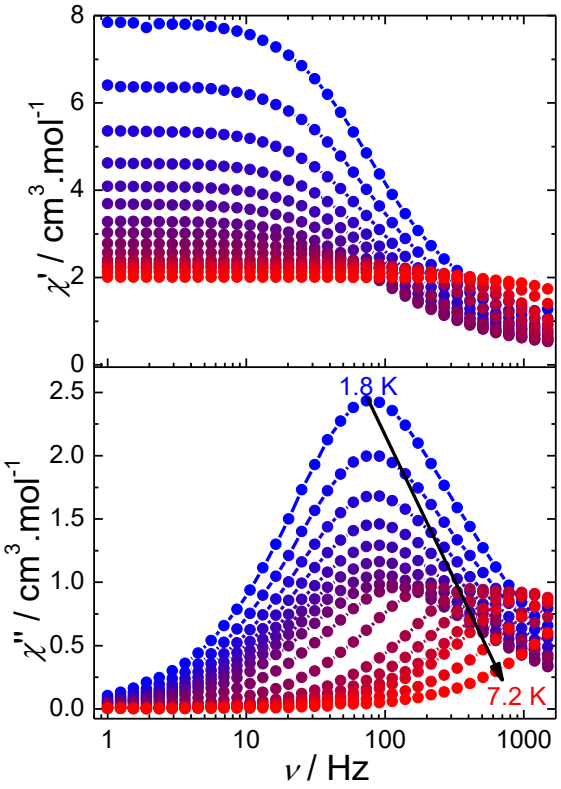

Fig. 2. Frequency dependence of the in-phase (χ') and out-of phase (χ'') susceptibilities for **1** under a zero dc-field.

The presence of a SMM behaviour was investigated by alternate current measurements. The frequency dependence of the ac susceptibility under a zero dc-field reveals the presence of a single frequency dependent maximum in the out-of-phase susceptibility (χ'') component indicating a slow relaxation of the magnetization (Fig. 2). Cole-Cole plots (Fig. S3) shows well-defined semi-circles which can be fitted with a generalized Debye model giving α parameter values ranging from 0.009 to 0.266 indicating a narrow distribution of relaxation times (Table S2). The increase of χ''observed at low temperature on the temperature dependence of χ'' (Fig. S4) points out the presence of a QTM, which is further confirmed by monitoring the temperature dependence of the relaxation time, τ, which becomes temperature independent at low temperature (Fig. 3). Hence, the $\ln\tau$ *vs.* T^{-1} plot shows a clear deviation from the linearity at low temperature confirming the presence of other relaxation processes. Consequently, the overall data range could be modelled using the following equation: $\tau^{-1} = \tau_0^{-1}\exp(-\Delta/kT) + CT^m + \tau^{-1}_{QTM}$ (Eq. 1).[25] The first term accounts for a thermally activated process, while the second and third ones stand for two-phonon Raman and QTM, respectively. The *m* value was alternatively fixed to 5 (best fit) or 9, which are the possible values observed for Kramers ions.[26] The best fit parameters gives $\Delta = 58 \pm 1$ cm^{-1}, $\tau_0 = (4.1 \pm 0.9) \times 10^{-10}$ s, $C = 0.038 \pm 0.008$ $s^{-1}.K^{-5}$ and $\tau_{QTM} = 1.68 \pm 0.03$ ms, indicating that the magnetization relaxes through a combination of these three processes.

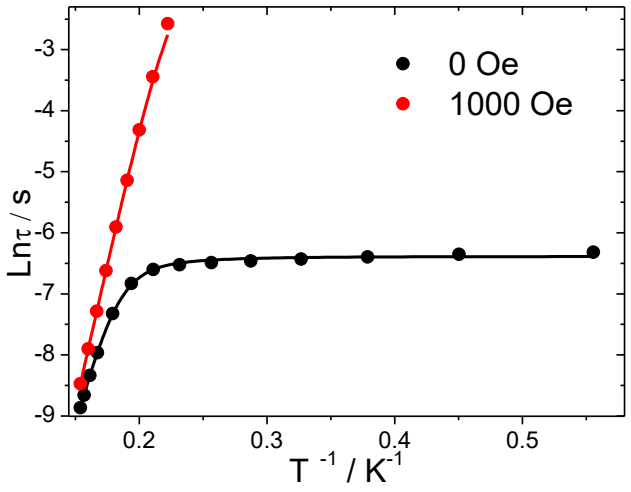

Fig. 3. Temperature dependence of the relaxation time for **1** using the ac susceptibility data at 0 Oe and 1000 Oe. The solid line represents the fit with Eq. 1 (0 Oe) and Eq. 3 (1000 Oe).

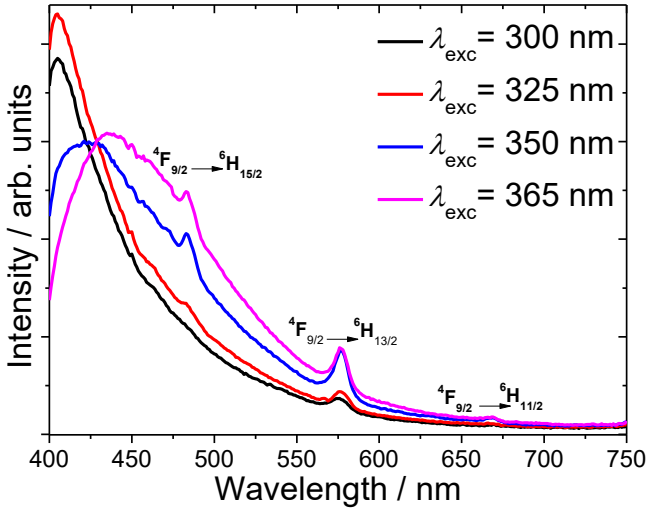

Fig. 4. Room temperature solid-state emission spectra of **1** acquired at different excitation wavelengths. The intra $4f^9$ Dy^{3+} transitions are reported.

To go further, the significant QTM could be shortcut by applying dc-field. As a consequence, the field dependence of the relaxation time at 6 K reveals the usual shape, which can be modelled with the equation $\tau^{-1} = DH^4T + B_1/(1+B_2H^2) + K$ (Eq. 2), for which the first term accounts for the direct process (for Kramers-ion), the second one for the QTM, while the K constant accounts for the field-independent Raman and thermally activated processes. The best fit parameters could be found in Table S3, while the optimum field (field at which the relaxation time is the highest) is in the range 1000-2000 Oe. The frequency dependence of the ac susceptibilities under a 1000 Oe field (Fig. S6) validates the reduction of the QTM, while the fitting of Cole-Cole plots (Fig. S7, Table S4) still shows low values of the α parameter (< 0.080) indicating a narrow distribution of the relaxation times. Fitting of the temperature dependence of the relaxation time could be performed with the following model: $\tau^{-1} = \tau_0^{-1}\exp(-\Delta/kT) + CT^m + AT$ (Eq. 3) (Fig. 3) in which the third term accounts for the direct process leading to the following fit parameters: $\Delta = 65.2 \pm 0.2$ cm^{-1}, $\tau_0 = (1.145 \pm 0.002) \times 10^{-13}$ s, $C = 0.004 \pm 0.002$ s^{-1}.K^{-5} (the A parameter is found negligible).

All these results point out a modest value of the anisotropic barrier, which could be rather surprising giving the quasi-linearity of the Cl-Dy-Cl sequence. Evaluation of the orientation of the anisotropic axes from the MAGELLAN[27] software based on electrostatic considerations and for both independent complexes confirms that this latter is directly oriented along the Cl-Dy-Cl string with anisotropic axis-Dy-Cl angle of around 2.0 and 0.4° for Dy1 and Dy2 sites, respectively (Fig. S8).

Although the negatively charged chloride anions in the *trans* position impose the orientation of the anisotropic axis from a pure electrostatic point of view, the presence of strongly interacting oxygen in the pentagonal plane provides a transverse magnetic anisotropy component and therefore a decrease of the overall anisotropy, which explains the modest value of the anisotropic barrier. Additionally, the relatively weak crystal-field generated by the chloride ions may not be able to afford a large m_J splitting. However and by comparison, a benzoquinone(BQ)-bridged dinuclear dysprosium complex $[BQDy_2Cl_2(THF)_6]$ showing a close environment with respect to **1** does not exhibit a slow relaxation of its magnetization due to the strong equatorial field imposed by the BQ ligands that induces a rotation of the magnetic axis in the basal plane.[22] On the other hand, a dysprosium complex based on a tridentate NCN pincer ligand $[Dy(NCN)Cl_2(THF)_2]$ with two chlorides in *trans* configuration shows an SMM behavior with a relaxation through the second excited state. In this example the magnetic axis is imposed by a strong Dy-C interaction within the equatorial plane.[21]

The optical properties of **1** were investigated. The absorption spectrum of **1** in THF shows a broad band at 270 nm and ascribed to the $\pi^* \leftarrow \pi$ transitions of the $[B(Ph)_4]^-$ moiety (Fig. S9).[28] Then, the photoluminescence properties of **1** were investigated in solid state. The room temperature emission spectra acquired at different excitation wavelengths show a dual luminescence constituted by an excitation dependent broad band in the 410-435 nm region and the typical Dy^{3+}-based luminescence at 485, 577 and 668 nm. The former broad band most likely originates from the tetraphenylborate moiety. Noticeably, the luminescence of tetraphenylborate salts is known to be relatively complex since this arises from the formation of excitons.[29-30] The excitation spectrum (Fig. S10) monitored in the intra $4f^9$ $^4F_{9/2} \rightarrow {}^6H_{13/2}$ Dy^{3+} transitions reveals the presence of sharp lines at 325, 350 and 365 nm pointing a direct sensitization within the 4*f* *transitions*. In addition, a broad excitation band ascribed to the $[B(Ph)_4]^-$ entity could be also observed at 300 nm. Lowering the temperature (77 K) results in the increase of the relative

intensities of the Dy^{3+}-based luminescence with respect to the broad emission band. These results indicate therefore than **1** exhibit a characteristic dual luminescence.

In conclusion, a simple dysprosium pentagonal bipyramidal complex exhibiting a linear Cl-Dy-Cl arrangement reveals a slow relaxation of the magnetization associated with a genuine SMM behaviour and a dual luminescence making the compound a bifunctional system. Despite the linear arrangement, a relatively modest anisotropic barrier was observed, which can be directly related to the presence of strongly coordinated THF solvates in the pentagonal plane that decrease the anisotropy. Yet, substitution of such solvates with softer Lewis bases may greatly enhance the magnetic properties.

Conflicts of interest

There are no conflicts to declare.

Acknowledgements

The financial support of the Russian Science Foundation is highly acknowledged (Project № 17-73-30036). The French authors thank the University of Montpellier, CNRS and PAC of ICGM.

Notes and references

1 R. Sessoli, H. L. Tsai, A. R. Schake, S. Wang, J. B. Vincent, K. Folting, D. Gatteschi, G. Christou and D. N. Hendrickson, *J. Am. Chem. Soc.*, 1993, **115**, 1804-1816.
2 R. Sessoli, D. Gatteschi, A. Caneschi and M. A. Novak, *Nature*, 1993, **365**, 141.
3 D. N. Woodruff, R. E. P. Winpenny and R. A. Layfield, *Chem. Rev.*, 2013, **113**, 5110-5148.
4 J. Tang and P. Zhang, in *Lanthanide Single Molecule Magnets*, Springer Berlin Heidelberg, Berlin, Heidelberg, 2015, DOI: 10.1007/978-3-662-46999-6_2, pp. 41-90.
5 R. A. Layfield and M. Murugesu, *Lanthanides and Actinides in Molecular Magnetism*, Wiley, 2015.
6 L. Ungur and L. F. Chibotaru, *Inorg. Chem.*, 2016, **55**, 10043-10056.
7 J. Luzon and R. Sessoli, *Dalton Trans.*, 2012, **41**, 13556-13567.
8 F. Troiani and M. Affronte, *Chem. Soc. Rev.*, 2011, **40**, 3119-3129.
9 L. Bogani and W. Wernsdorfer, *Nat. Mater.*, 2008, **7**, 179-186.
10 J. D. Rinehart and J. R. Long, *Chem. Sci.*, 2011, **2**, 2078-2085.
11 L. Escalera-Moreno, J. J. Baldoví, A. Gaita-Ariño and E. Coronado, *Chem. Sci.*, 2018, **9**, 3265-3275.
12 N. F. Chilton, *Inorg. Chem.*, 2015, **54**, 2097-2099.
13 J. Liu, Y.-C. Chen, J.-L. Liu, V. Vieru, L. Ungur, J.-H. Jia, L. F. Chibotaru, Y. Lan, W. Wernsdorfer, S. Gao, X.-M. Chen and M.-L. Tong, *J. Am. Chem. Soc.*, 2016, **138**, 5441-5450.
14 S. K. Gupta, T. Rajeshkumar, G. Rajaraman and R. Murugavel, *Chem. Sci.*, 2016, **7**, 5181-5191.
15 M. Gregson, N. F. Chilton, A.-M. Ariciu, F. Tuna, I. F. Crowe, W. Lewis, A. J. Blake, D. Collison, E. J. L. McInnes, R. E. P. Winpenny and S. T. Liddle, *Chem. Sci.*, 2016, **7**, 155-165.
16 Y.-C. Chen, J.-L. Liu, L. Ungur, J. Liu, Q.-W. Li, L.-F. Wang, Z.-P. Ni, L. F. Chibotaru, X.-M. Chen and M.-L. Tong, *J. Am. Chem. Soc.*, 2016, **138**, 2829-2837.
17 Y.-S. Ding, N. F. Chilton, R. E. P. Winpenny and Y.-Z. Zheng, *Angew. Chem. Int. Edit.*, 2016, **55**, 16071-16074.
18 Y.-S. Meng, L. Xu, J. Xiong, Q. Yuan, T. Liu, B.-W. Wang and S. Gao, *Angew. Chem. Int. Edit.*, 2018, **57**, 4673-4676.
19 F. S. Guo, B. M. Day, Y. C. Chen, M. L. Tong, A. Mansikkamaki and R. A. Layfield, *Angew. Chem. Int. Ed. Engl.*, 2017, **56**, 11445-11449.
20 C. A. P. Goodwin, F. Ortu, D. Reta, N. F. Chilton and D. P. Mills, *Nature*, 2017, **548**, 439-442.
21 Y.-N. Guo, L. Ungur, G. E. Granroth, A. K. Powell, C. Wu, S. E. Nagler, J. Tang, L. F. Chibotaru and D. Cui, *Sci. Rep.*, 2014, **4**, 5471.
22 J. O. Moilanen, A. Mansikkamäki, M. Lahtinen, F.-S. Guo, E. Kalenius, R. A. Layfield and L. F. Chibotaru, *Dalton Trans.*, 2017, **46**, 13582-13589.
23 S. Anfang, K. Dehnicke and J. Magull, *Z. Naturforsch., B: Chem. Sci.*, 1996, **51**, 531-535.
24 D. Casanova, M. Llunell, P. Alemany and S. Alvarez, *Chem. Eur. J.*, 2005, **11**, 1479-1494.
25 K. R. Meihaus, S. G. Minasian, W. W. Lukens, S. A. Kozimor, D. K. Shuh, T. Tyliszczak and J. R. Long, *J. Am. Chem. Soc.*, 2014, **136**, 6056-6068.
26 P. L. Scott and C. D. Jeffries, *Phys. Rev.*, 1962, **127**, 32-51.
27 N. F. Chilton, D. Collison, E. J. L. McInnes, R. E. P. Winpenny and A. Soncini, *Nat. Commun.*, 2013, **4**, 2551.
28 R. T. Pflaum and L. C. Howick, *Anal. Chem.*, 1956, **28**, 1542-1544.
29 M. Gouterman and P. Sayer, *J. Mol. Spectrosc.*, 1974, **53**, 319-335.
30 V. A. Nadolinnyi, O. V. Antonova, A. A. Ryadun, E. A. Il'inchik, V. V. Korolev and O. P. Yur'eva, *Doklady Physical Chemistry*, 2010, **432**, 92-95.